Accepted refereed manuscript of: Usai MR, Pickering MD, Wilson C, Manunza MR, Garbi I, Pittoni E, Brothwell DR & Keely BJ (2018) Evidence from burial sediments for prehistoric burial practice and ritual in Monte Claro chambered tombs: Micromorphology, mineralogy and geochemistry. *Journal of Archaeological Science*, 100, pp. 139-147. DOI: https://doi.org/10.1016/j.jas.2018.10.008.

Evidence from burial sediments for prehistoric burial practice and ritual in Monte Claro chambered tombs: micromorphology, mineralogy and geochemistry

Maria Raimonda Usai[a,b,1], Matthew D. Pickering[c], Clare Wilson[d], Maria Rosaria Manunza[e], Ilaria Garbi[f], Emanuele Pittoni[f], Don R. Brothwell[a1] and Brendan J. Keely[c]*

[a]Department of Archaeology, University of York, King's Manor, Exhibition Sq. York YO1 7EP

[b]Dipartimento di Architettura e Design, Wilson, Piazza Pau Salit, Alghero, Italy

[c]Department of Chemistry, University of York, Heslington, North Yorkshire, YO10 5DD

[d]School of Biological and Environmental Science, University of Stirling, Stirling. FK9 4LA UK

[e]Soprintedenza ai Beni Archeologici, Piazza Indipendenza 7, 09100 Cagliari, Italy

[f]Via Stradella 62, 09045 Quartu S.Elena, Cagliari, Italy

ORCID ID

Keely: 0000-0002-8560-1862

Pickering: 0000-0002-6234-2108

Wilson: 0000-0002-0287-8576

*Corresponding author

Email: brendan.keely@york.ac.uk

Tel: +44(0)1094 322540

Highlights

- Signatures present in burial sediments can aid interpretation of human burials
- Ca depletion in sediments underlying disarticulated remains indicative of primary burial
- Reddish deposit identified as being ochre applied to the grave
- The silicified remains of a sedge torch reveal how the burial chamber was illuminated

[1] Deceased 13 May 2018 (MRU) and 26 September 2016 (DRB)

Abstract

The burial matrix in archaeological graves is seldom subject to detailed examination for evidence of its potential interaction with the interred remains. Sediments adjacent to skeletal remains resting on a marl platform in a subterranean chambered burial dated to the third millennium BC were investigated using micromorphological, archaeobotanical, and chemical methods. Micromorphological features in the tombs, typical of $CaCO_3$ depletion, appeared more abundant in positions close to the skeletal remains than in positions further away, suggesting that the carbonate dissolution was caused by acidification resulting from the body decay as well as from environmental factors. Organic signatures around the remains were dominated by background sedimentary organic matter of the marl, attesting to the exposed style of burial being unfavourable for the preservation of organic remains. Red concentrates present in a distinct region of the resting platform were distinguishable from similar coloured deposits formed by debris from the vault. They were identified as haematite (ochre) deposits, matching features observed in other prehistoric sites, including those of the same culture, and attesting to ritual associated with the treatment of the dead. Greyish fibrous contexts found on the burial resting platforms were identified as silicified sedge, probably remnants of the combustible parts of torches. The position and nature of the sedge-derived material suggests their use for illuminating the graves at depth and/or as a possible votive ritual. The detailed scientific examination of the burial matrix can reveal unique perspectives and add interpretative value to the archaeological investigation of graves.

Keywords: Eneolithic chambered burials; geoarchaeology and micromorphology; organic geochemistry; ochre; ritual burning.

1 Introduction and site description

The InterArChive project considered the extent to which the burial matrix preserves evidence that is currently unexploited within the archaeological investigation of human burials (Usai et al. 2014). Soils/sediments originating from a diverse range of temporal and geographical contexts were examined using systematic sampling and a multidisciplinary analytical approach (Burns et al. 2017; Pickering et al. 2014, 2018; Usai et al. 2014). One of the sites examined, Gannì, Sardinia, belongs to the Eneolithic Culture of Monte Claro, a culture that displays intriguing signs of ritual burial practices (Manunza 2010a, 2010b; Ugas 1993). The culture was named after discovery, in 1906, of an Eneolithic burial in the Monte Claro area within the city of Cagliari. The burial contained a stone bench as a resting platform for the dead, and various grave goods including a situlate vessel and a *monoansato* (single handled) bowl. In this, and other Monte Claro tombs discovered later, the primary deposition of the dead was in a crouched position on their left side with features ascribed to ochre in some of

57 the graves. The practice of adorning ancient graves with ochre has been described for archaeological
58 sites as far back as Palaeolithic age (Roebroeks et al. 2012), the deep red colouration in burials from
59 various sites and periods being attributed to haematite (Gialanella et al. 2011; Roebroeks et al. 2012).

60 Two underground chambered Copper Age burials of the Eneolithic Culture of Monte Claro, at the
61 archaeological site of Gannì (Fig. 1a, b), presented a unique opportunity to examine the evidence for
62 ritual burial practices within this culture. The vaults, carved into the massive Miocene bedrock
63 (Carmignani et al. 2012) using prehistoric implements (Fig. 2a), extend to *c.* 3 m underground. Tomb
64 I contained two burial chambers (T1 and T2) whereas Tomb II was constructed with a small entrance
65 vestibule connected to a single burial chamber (Fig. 2b). Tomb II contained human skeletal remains
66 radiocarbon dated to 2469-2293 BC (Manunza 2013). Tomb II and chamber T2 of Tomb I were found
67 fully sealed and unviolated, and hence with all architectural elements in place. The archaeological
68 features of the tombs and their cultural implications have been described by Manunza (2013).

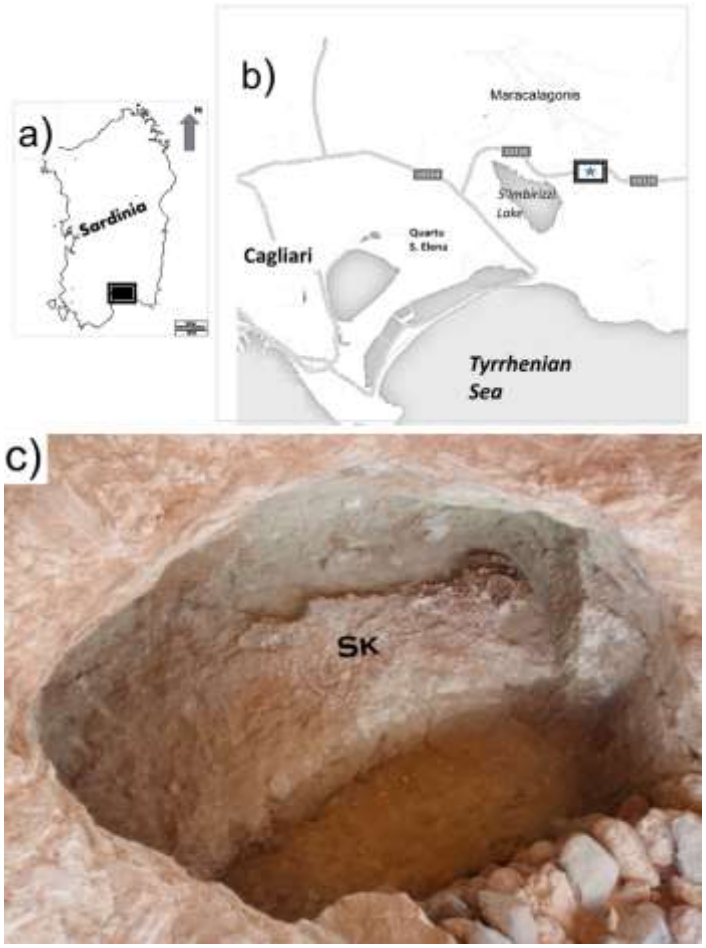

69

70 Fig. 1. a) Location of the site in Sardinia (black rectangle); b) inset corresponding to the black rectangle
71 in a): site location is indicated by the star; c) close-up of the burial chamber of Tomb II with position
72 of skeletal remains indicated by the letters Sk.

The Gannì graves feature sub-vertical access tunnels leading from the land surface to underground burial chambers delimited by small stone walls and stone benches employed as resting platforms for the dead (Fig. 1c). Such architecture was frequent in Monte Claro burials in Sardinia and also among coeval cultural groups of Aegean-Anatolian background in central-southern Italy. The former include sites some distance from Gannì as well as others that are closer to the site (Table S1).

At the time of sampling, the skeletal remains in Chamber T1 of Tomb I at Gannì were disarticulated, having been disturbed by thieves. Prior to the disturbance, Chamber T1 contained disarticulated and damaged bone as well as the skeletons of a male and a female aged between 18 and 25 years and two males aged 30-45 and 20-30 years resting on stone benches. In the second, unviolated chamber, T2, the remains of two children rested in a niche in the wall and, directly on the floor below, were the skeletons of a male and female couple (aged 18-25 years) next to a child aged 9-10 years. Tomb II, fully sealed and unviolated, contained poorly-preserved skeletal remains of an adult female aged 35-50 years in anatomical position, lying crouched on the left side and resting on a bench carved in the marl (Fig. 3). Archaeological interpretation suggested that the burials date to the Monte Claro culture (Manunza 2013). The absence of bone lesions excluded interpersonal violence as causes of death, suggesting a local epidemic or, more likely given the patterns of articulation, that these were sites of collective burials (Manunza 2013).

Fig. 2. a) Internal vault of Tomb II carved with prehistoric implements during the Copper Age; b) front vestibule of Tomb II connecting to burial chamber through a small stone wall (see Fig. 1c for close-up).

The positioning of individuals either on stone-carved benches or in direct contact with the floor at Gannì, and also in the Cagliari, Selargius, Settimo and Serdiana sites, has been interpreted to relate to social status – tombs where additional efforts were expended to fashion stone benches were postulated to have been destined for people of higher status (Manunza 2013). An emergent group of high status within the local community was also suggested by the exceptional quality of some of the

pottery present in Tomb I (Manunza 2013). This included bowls decorated by incisions, plates, vases with polished surfaces, cups, beakers, situlate vessels and fragments of vases. The pottery was similar to that found at many other Monte Claro sites, the *situlae* being very similar to those found in sites South of the S'Imbirizzi Lake and in Cagliari. Vessels and *monoansato* bowls from Gannì were also very similar to those of the first Monte Claro burial excavated in Cagliari, particularly in the shape of the rims and identical decoration of the bowls. Other fragments of ceramics had identical decorations to those of a site near Villasor. A stone axe, three-pointed stone tool and a pointed copper implement were also found. The grave goods were all from Tomb I, no grave goods were present in Tomb II, and their features were not sufficient to determine whether they were part of any particular burial practice or ritual at the site.

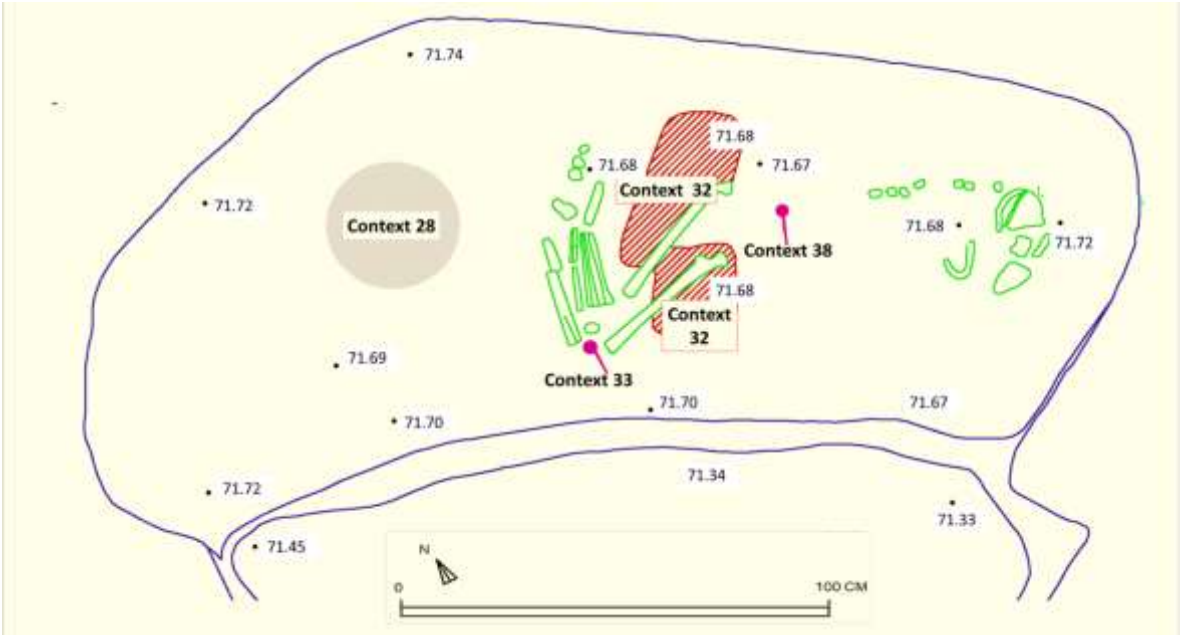

Fig. 3. Plan of Tomb II resting platform, with context and sample distribution (notations in Table S2; height expressed in metres above sea level). The skeletal remains (green in colour image) were orientated NW-SE with the skull to the south east.

The vault marl, of dominant colour in the yellow-red range (2.5YR8-7/1-2) (Munsell 2009), contained variable amounts of orange-coloured deposition nodules. Much of the bone in Tomb II had been lost due to decay and the skeletal remains and the platform on which they rested (Fig. 3) were covered in places by sparse sediment deposits, tentatively interpreted on site as debris fallen from the vault. The debris displayed several colours in the yellow-red range (2.5YR7-6/3-4) (Munsell 2009) and rare fine bio-voids and cracks were visible to the naked eye. Fine rock fragments and poorly developed soil aggregates (peds), barely visible at field scale, suggested a low degree of pedogenesis. Two visually

distinct areas of the resting platform, one red-coloured (Context 32) and the other grey (Context 28), were evident (Fig. 3).

1.1 Deep red concentrates

Concentrates of very deep red colour, varying in the range 2.5YR 8-5/3-4 (Munsell 2009), were situated in the vicinity of the pelvis and thighs of the skeleton in Tomb II (Context 32; Fig. 3). The material appeared as a covering over part of the resting platform and as deposits with sharp or diffuse boundaries over bone fragments and the local rock/sediment components (Fig. 4). Preliminarily on-site interpretation was that the material could be ochre (Manunza 2013), as observed in other ancient burials (Roebroeks et al. 2012).

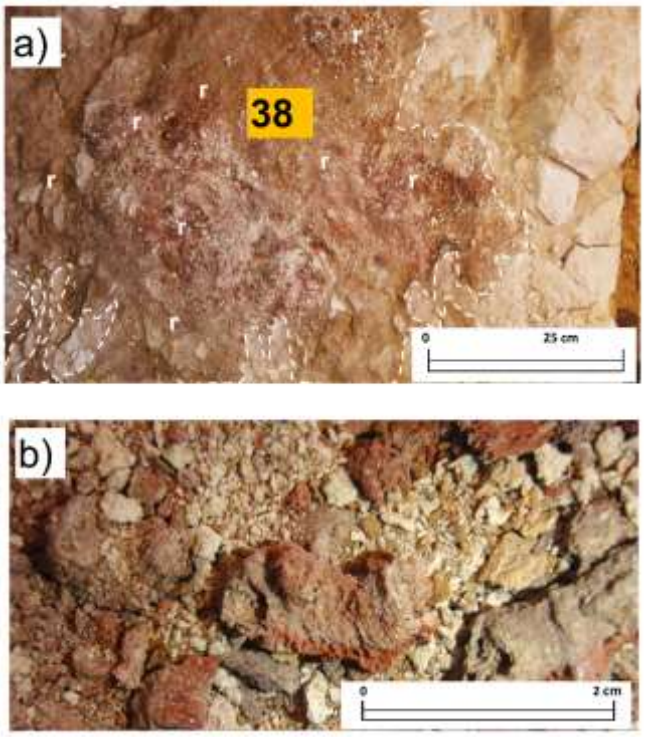

Fig. 4. a) Photograph of Context 32, comprising a deep red material (area marked by 'r' and enclosed by white outline); b) detail of the red material showing the intense red feature indicated with 'r' in a).

1.2 Fibrous grey contexts

Loose grey material was found near the presumed position of the feet in Tomb II (Context 28 in Fig. 3), forming a thin, irregular, sub-circular lens over the resting platform (Fig. S1). A visually similar material was present in a clump to the side of and between the two burial platforms in Chamber T1 of Tomb I (Context 13). Visual inspection revealed the material to include fine fibrous filaments; its nature and possible ritual implications was unclear from field and macro-scale observations.

The nature, chemical and mineralogical compositions of two coloured pedofeatures in Context 32 and of the grey fibrous material of Contexts 13 and 28 were examined to determine their compositions and significance in relation to the grave sediments, burial practices and effects of body decomposition on the burial matrices that had been adjacent to and beneath the skeletal remains.

2 Methods

2.1 Sampling

The sampling protocols for the InterArChive project (Usai et al. 2014) were followed as closely as possible given the limitations of the incomplete nature of the skeletal remains (Fig. 3, Table S2). Undisturbed sediment samples were collected with Kubiena tins or hand lifting, each with a loose replicate. Site controls were collected from the marl surrounding the grave: from the sides, C1(α), and from a marl bed equivalent to the resting platform from the vault in Tomb II, C1(β) (Carmignani et al. 2012). Control C4 was collected from the thin layer deposited on top of the skeletal remains in Tomb II. The sediments from the skull and pelvic regions were collected from the upper part of the resting platform under the skeletal remains. Loose sediment samples for organic chemical analysis were collected from numerous positions around the skeletal remains (Table S2) and from the red and grey contexts. Thin sections were analysed from the block-lifted undisturbed samples. They were examined by light microscopy and scanning electron microscopy-energy dispersive X-ray spectroscopy (SEM-EDS). Loose sediment samples were dried, sieved and aliquots of selected samples subjected to X-ray diffraction (XRD). Aliquots were also subjected to total organic carbon analysis and extraction with organic solvent to recover organic residues. The organic residues were derivatised and analysed by gas chromatography-mass spectrometry (GC-MS). Full experimental details are given in SI.

3 Results and discussion

3.1 Micromorphology and inorganic chemistry

3.1.1 Grave and site controls

The material overlying the skeleton (Control C4) was visually and compositionally similar to the marl of the vault, though with some evidence of pedogenesis, consistent with debris originating from the chamber vault rather than being from allochthonous material that was intentionally deposited on the skeleton. Thus, the C1 controls, representing the marl from which the vault was excavated, exhibited largely uniform groundmass with *c.* 50% grey and crystallitic fine material (≤ 2 μm) and a coarser fraction (mainly ≤ 50 μm grains but occasionally as grains and composite silt agglomerates of up to 200 μm). The orange-coloured nodules observed on-site in the grave vault were not observed in the thin sections from C1(β), probably as a result of local variability. Voids in the controls were mostly planar, randomly oriented and typical of rock fracturing. Quartz and calcite were both very well

represented in XRD analysis of the vault control C1(β) (Fig. S2). Control C4 showed evidence of pedogenesis through the presence of 2 - 200 μm granular peds (80% of slide area), sub-angular blocky peds and small randomly orientated biovoids. Orange-coloured nodules observed in thin section reflect material derived from the vault.

3.1.2 Debris on resting plane (Contexts 32, 37 and 38)

The samples from the resting platform, while exhibiting compositional features consistent with derivation from the marl, showed limited evidence of pedogenesis and alteration. Thus, within the upper *c.* 10 mm the deposits under the pelvis (Context 38) and the red area adjacent to it (Context 32), rare, very small and poorly developed peds were observed (Fig. S3). Voids with sub-parallel orientation to the resting platform and cloudy crystallitic *b*-fabric only in the regions under the skull (Context 37) and pelvis (Context 38) reflect pedogenic processes in areas contiguous to the skeletal remains, *i.e.* in the upper *c.* 10 mm of areas of the resting platform below the skeleton.

3.1.2.1 Pedofeatures T and R

The debris coating the upper 10 mm of the surface of the resting platform contained two distinct pedofeatures, designated T and R. The debris was disturbed beneath the thigh (Context 32) and pelvic regions (Context 38). Pedofeature T was compositionally similar in both areas and dominated the samples. Its chemical composition and anatomical location are consistent with decalcified marl formed by leaching due to generation of acidic fluids during decomposition of the body. Specifically, pedofeature T, beige (PPL) and frequently isotropic or dark grey in XPL exhibited lower crystallinity than the groundmass (Fig. 5). Abundance levels were ≥ 50% of the thin section areas throughout the upper 8 mm of the resting platform, with a sharp decrease to almost 0% at 8 mm depth but occasionally extending further down to 20 mm depth (Fig. 5). SEM-EDS revealed that pedofeature T in the thin sections from Contexts 32 and 38 showed no significant difference in elemental composition, suggesting similar origins or processes of formation in both contexts. Pedofeature T was dominated by Si and Al together with Fe, K, and trace amounts of Na, Mg, P and S (Table S3). The Fe contents were higher, and Ca substantially lower, than in the adjacent grey matrix in the thin section and in the C1(β) control (Table S3). XRD analysis indicated that Context 38 exhibited significantly depleted calcite levels relative to the marl of the vault. Given that the micromorphology and depth profiles of pedofeature T suggest that it formed as an alteration product rather than as a surface deposit, the chemical composition was compared with that of the unaltered grey fabric of the resting platform (Table S3). As with the vault control, the grey fabric was dominated by Ca, the levels being much higher and Si, Al and Fe being lower than in pedofeature T (Table S3). To account for decalcification, the data were normalised to the Si content, enabling direct comparison of pedofeature

T and the grey matrix (Fig. 6). The significantly lower Ca and Mg contents and slightly higher, but statistically significant, Fe content is consistent with pedofeature T being formed by depletion of the grey matrix. The prevalence of pedofeature T in the deposit directly under the pelvis hints at the depletion being caused by generation of acidic fluids during decomposition of the body, consistent also with the lower prevalence under the skull.

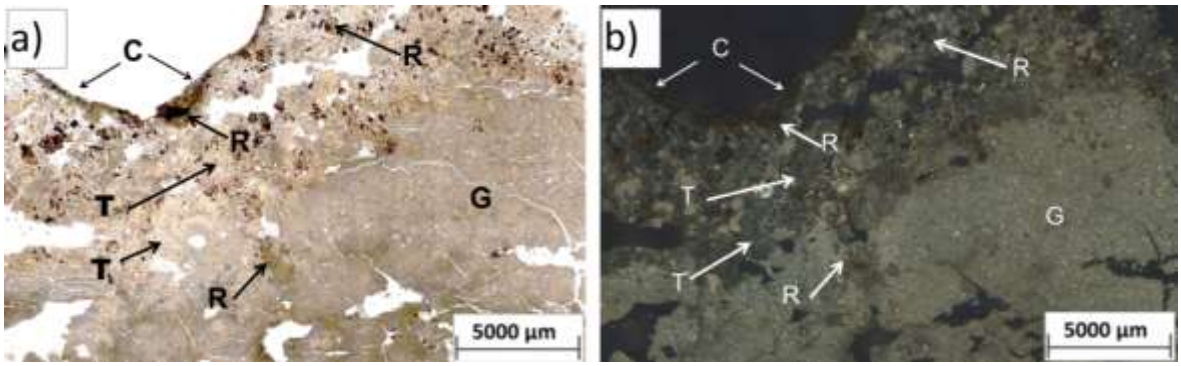

Fig. 5. Mosaic image comprising all adjacent fields of view from the thin section from Context 32: a) PPL, pedofeature R comprises deep to very light red opaque material and b) XPL. Pedofeature T appears black or very dark. The bulk of pedofeature T appears as a disturbed zone of lower crystallinity situated under the sub-horizontal resting plane (toward the upper part of the image). A small cavity within the sub-horizontal resting plane is denoted C. The grey matrix (G) appears mostly in the lowermost part of the section (as also observed in Context 38).

Pedofeature R, deep to very light red opaque material (Figs 3 and S4), was generally adjacent to pedofeature T (Fig. 5). The abundance levels dropped sharply from *c.* 10% area in the uppermost 7-11 mm of the resting plane in Context 32 to only occasional occurrences below 7-11 mm depth. Context 38 contained a few fragments of pedofeature R below the pelvic bone. The material differs chemically from the marl of the vault and was identified as haematite, consistent with ochre deposits added to the surface of the resting plane. Specifically, the material of the reddened area of the resting platform (Context 32) contained isolated micro-patches of Fe oxides of variable colour intensity in thin section (Fig. S4). The accumulations (ranging from 10 to 150 µm) were interpreted as weakly to strongly impregnated nodules and occasionally as fragmented typic- or hypo-coatings.

Pedofeature R in Context 32 exhibited an appreciable content of silica as revealed by SEM-EDS analysis (Si = 10.2%) and the Fe contents of the red particles were highly variable (Table S3). The low concentrations of Al, Ca and Mg suggest relatively low levels of aluminosilicate and carbonate components by comparison with the vault control and grey matrix in the undisturbed samples from

the resting platform (Table S3). XRD analysis indicated these deep red components to be composed mainly of haematite, consistent with ochre deposits: goethite was not detected in any of the samples (Fig. S2). The similar levels of quartz and calcite in the host materials (Fig. S2) suggest similar mineral types, sizes and orientations. Hence, it is likely that the intensity of the secondary XRD radiation correlates with differences in amounts of mineral species present. Thus, the depth distribution, disturbed nature, chemistry and morphology of the pedofeature is consistent with an allochthonous material deposited on the surface of the resting platform and incorporated into the disturbed/debris layer to a depth of *c.* 11 mm.

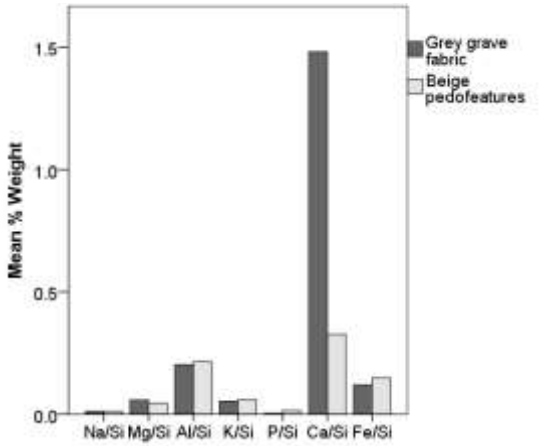

	***p*-value (ANOVA)**[237]
Ca/Si	< 0.000*
Fe/Si	0.037*
P/Si	0.348
K/Si	0.218
Al/Si	0.396
Mg/Si	0.008*

Fig. 6: Comparison of relative element abundances in beige pedofeature T and grey grave *b*-fabric. Significance threshold = 0.05.

3.2 Grey fibrous material (Contexts 13 and 28)

Microscopy revealed the dominant material of the grey fibrous deposit of Context 13 to contain recognisable remains of plant material. When concentrated by acid dissolution of carbonate, characteristic features of Poales (grasses and sedges) could be recognised. The plant remains were preserved mainly as silica, consistent with the material having been burnt *in situ*. Specifically, under low-power microscopy, the grey fibrous material of Context 13 appeared to include two components: a minor one comprising tubular structures (*c.* 15 mm × 2 mm), possibly parts of recent roots, and a major component comprising finely divided amorphous granules and powdery material. The latter, also present in Context 28, contained bright white spicules with maximum dimension up to about 4 × 0.5 mm but mostly about 2 × 0.25 mm. Treatment of unconsolidated replicates of Context 13 with hydrochloric acid revealed that the granules and powder were highly calcareous whereas the spicules remained undissolved. At ×400 magnification the spicules were recognisable as fragments of plant epidermis in the form of silica skeletons, where the original cell walls had been replaced by silica. Most specimens bore typical epidermal features of Poales (grasses and sedges) in the form of long and short cells, the former with characteristic finely sinuous walls (Fig. 7a). Many fragments bore small 'prickles'

255 (micro-hairs) on their surfaces (Fig. 7a) and some bore more obvious and quite substantial marginal
256 teeth (Fig. 7b, c). Some fragments bore rows of stomata exhibiting the morphological characteristics
257 (elongated dumbbell shaped structures) associated with grasses and sedges (Fig. 7b). In other cases
258 the fragments appeared to be more or less cylindrical, with prominent teeth (Fig. 7d), and were
259 presumably from a bristle or awn from the tip of a leaf or from a spikelet within a flowering head.

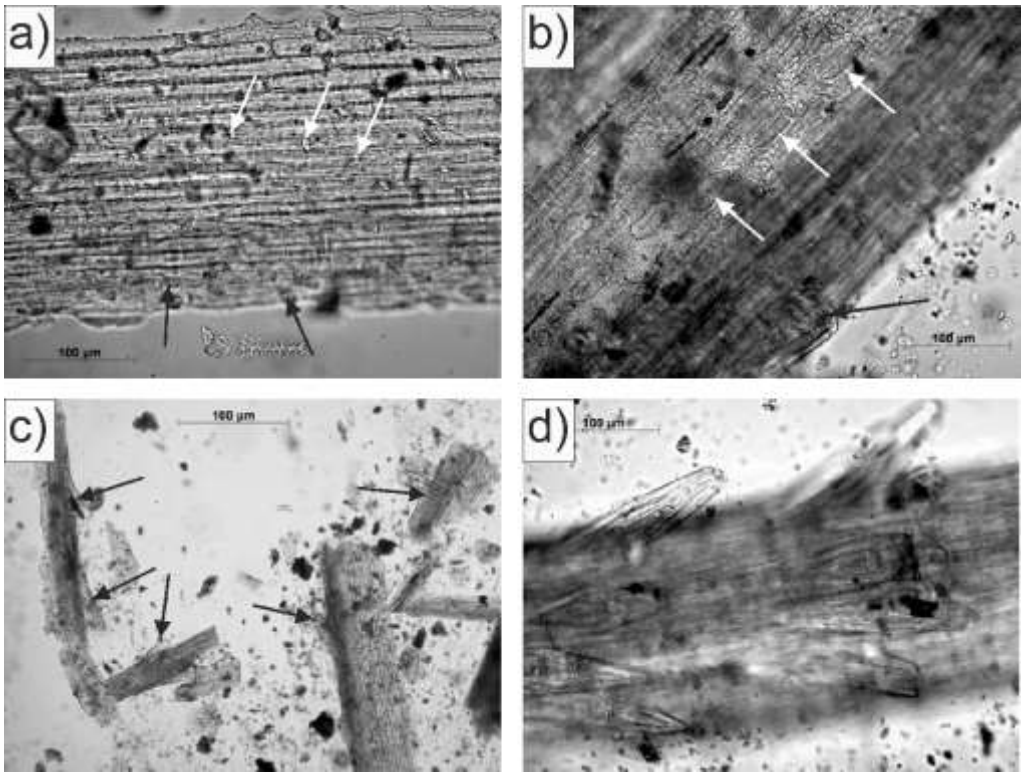

260

261 Fig. 7. Optical microscope (×400 magnification) images of silicified plant remains from Context 13.
262 Epidermis with a) long cells, short cells (white arrows) and prickles (black arrows). The single 'spiny'
263 structure at the bottom centre is a detached epidermal cell; b) marginal tooth (black arrow) and a row
264 of stomata (white arrows); c) sharp marginal teeth indicated by arrows; d) awn fragment with whorls
265 of teeth.

266 Further identification of the grey fibrous material was not possible in the absence of relevant
267 reference material though, on the basis of the tissue anatomy observed, only one or two taxa are likely
268 candidates. The size is rather small for one of the major cultivated grasses (*i.e.* cereals). Preservation
269 by silicification[2] has been observed occasionally in archaeological occupation deposits where it was
270 inferred that large quantities of silica-rich plant material had been burnt under strongly oxidizing

[2] Silicification is a term used in palaeobotany to denote permineralisation of tissues by silica within an aqueous burial environment, and this differs as a mechanism from what is presumed to have occurred in these archaeological specimens.

conditions, generating temperatures sufficient for the silica in the tissues to be fused, but low enough to prevent loss of cell structure (Robinson and Straker 1991). Such silicified material was attributed to rapid accumulation or burial of plant materials, protecting the delicate cellular structure from mechanical damage (Hall and Huntley 2007). Material of this kind in several prehistoric and medieval sites in England represented concentrations of cereal chaff (Robinson and Straker 1991) and, in several sites in Northern England, material other than cereal chaff was sometimes recorded (Hall and Huntley 2007). SEM-EDS analysis of the fibrous material in Context 28 confirms its siliceous nature (Table S3), consistent with silicified plant epidermis as suggested from palaeobotany. The XRD analysis indicated that calcite and quartz were scarce in the grey fibrous material of Context 28, contrasting with the high level of Si detected by SEM-EDS (Table S3) and calcareous component indicated by dissolution with acid. The apparent discrepancies are consistent with dominance of poorly ordered carbonate and silica (Drees et al. 1992) formed by a process, such as burning, that did not induce crystallisation. Hence, the components of Contexts 13 and 28 represent remains of leaf and flower parts from non-cultivated herbaceous materials that underwent silicification induced by fire. Given the delicate nature of the material and its form, the mineralisation must have occurred *in situ*.

3.3 Organic chemical analysis

With the exception of the grey material (Context 28) the organic carbon contents of the sediment samples from around the skeletal remains were not distinguishable from those of the controls suggesting there to be no significant contribution from the human remains. The absence of organic material associated with the coloured pedofeatures in Context 32 is consistent with its colour being due to haematite rather than to an organic dye. By contrast, Context 28 contained molecular signatures consistent with an origin from sedge. Specifically, total organic carbon (TOC) analysis revealed the majority of sediment samples from around the skeletal remains to be very similar to the controls, containing low levels of organic carbon (TOC values << 1%; Table S4) and with the majority of carbon being in the form of inorganic carbonate. By contrast, the grey material (Context 28) exhibited the highest TOC content (0.77%). GC-MS analysis of the total solvent extractable organic matter revealed the samples to contain organic compounds including $C_{16:0}$ and $C_{18:0}$ fatty acids, monoacylgycerols (MAGs), *n*-alkanols ($C_{18:0}$ and C_{24}-C_{30}), *n*-alkanes (C_{29} and C_{31}), β-sitosterol and cholesterol (Fig. 8), all present in low concentrations, consistent with the low organic matter contents indicated by elemental analysis. For the most part, little variation was evident between the lipid profiles of the controls (e.g. C1(β)) and samples taken from around the skeletal remains (e.g. Fig. 8a) suggesting they contain predominantly background sediment organic matter with little contribution from the human remains.

The extract from the grey deposit (Context 28) contained appreciable amounts of C_{22}-C_{32} *n*-alkanoic acids, C_{24}-C_{30} *n*-alkanols and β-sitosterol (Fig. 8b) together representing 6136 ng/g sediment, *cf*. 383 ng/g sediment for C1(β). The higher levels of those components in the grey deposit is indicative of a significant higher plant input (Eglinton and Hamilton 1967; Jambu et al. 1993). In addition, the profile includes two prominent peaks at retention times (t_R) 53.5 and 57.5 min (Fig. 8b), which do not feature in the other extracts and are comparable in abundance to sitosterol. GC-MS revealed their molecular ions ($M^{+\cdot}$) at *m/z* 548 and 576 and the same principal fragment ions: *m/z* 268 (base peak) accompanied by low abundance ions at *m/z* 267, 281 and 310 (e.g. Fig. 9). The EI mass spectra are characteristic of long chain alkylresorcinols (Avsejs et al. 2002). The ratio of *m/z* 268:267 of approximately 5:1 is consistent with the attachment of the alkyl chain at position 5 on the aromatic ring (Zarnowski and Kozubek 1999). Accordingly, the two components were assigned as 5-*n*-alkylresorcinols having C_{21} and C_{23} alkyl chains, respectively. The presence of a minor C_{19} alkyl homologue ($M^{+\cdot}$ = *m/z* 520) at t_R = 50.5 min (Fig. 8b) was revealed in the *m/z* 268 extracted ion chromatogram.

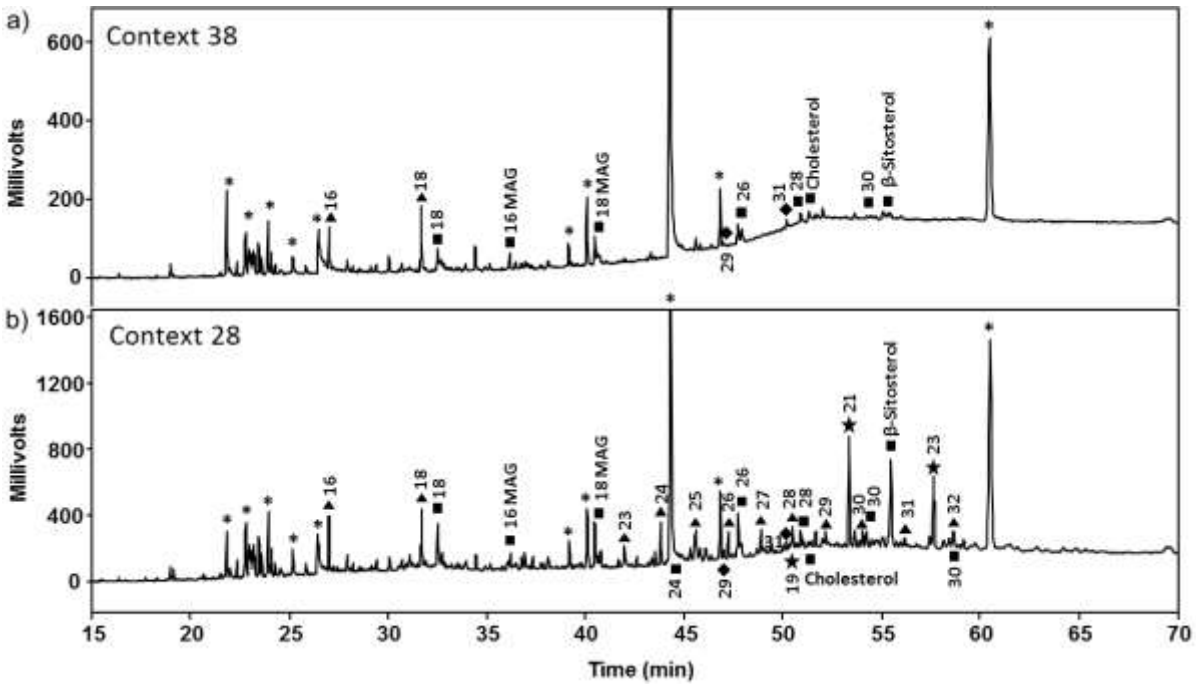

Fig. 8. Partial FID gas chromatograms of the total lipid extracts from a) the abdomen, Context 38, and b) the grey material, Context 28. Triangles = *n*-alkanoic acids, squares = alcohols (mainly *n*-alkanols unless labelled otherwise), diamonds = *n*-alkanes, stars = 5-*n*-alkylresorcinols, MAG = monoacylglycerols. Numbers denote carbon chain length. * = plasticisers arising from plastic bags used for sample storage.

Previous reports of 5-*n*-alkylresorcinols possessing alkyl chains in the range C_{13}-C_{27} and exhibiting a prevalence of odd-chain members indicate a range of natural sources including higher plants, algae, fungi and bacteria (Kozubek and Tyman 1999). Their biological function is largely uncertain although they are believed to fulfil roles including microbial resistance, growth regulation and membrane modulation (Kozubek and Tyman 1999). Cereals such as wheat and rye contain substantial amounts of alkylresorcinols. Previous studies, involving pollen analysis or examination of the contents of burial pots, have indicated foodstuffs, including cereals, as occasional items placed in human burials (Lagerås 2000). The 5-*n*-alkylresorcinol distributions of cereals, typically C_{17}-C_{25} and dominated by the C_{19} and C_{21} components (Chen et al. 2004; Mattila et al. 2005; Ross et al. 2003), do not match that of the grey context, whereas dominance of the C_{21} and C_{23} 5-*n*-alkylresorcinol homologues for the sedge *Rhynchospora alba* (Avsejs et al. 2002) represents a close match. The resorcinols and silicified remains indicate that the grey material associated with the burial is plant-derived, consistent with the visual description of a fibrous plant like material overlying the area from which the sample was collected. The survival of such clear indicators of plant remains after 4500 years of burial is remarkable, especially given their exposure to air and to combustion. The apparent recalcitrance of the 5-*n*-alkylresorcinols in that material could be due in part to their antimicrobial properties and may have extended protection to other biomarkers such as sitosterol.

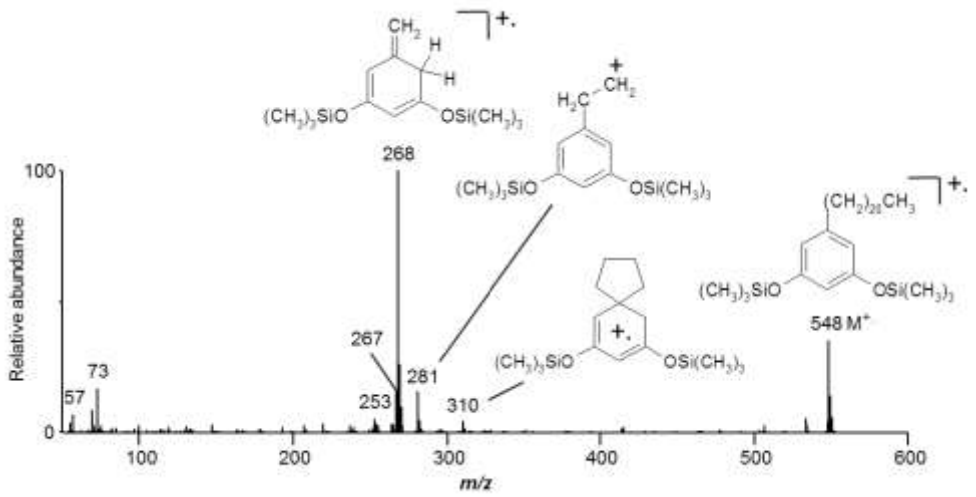

Fig. 9. Electron ionisation mass spectrum (70 eV) of C_{21} 5-*n*-alkylresorcinol.

As with the samples in close association with the skeletal remains, the total lipid extract from the red material (Context 32) is extremely similar to those of the controls. The solvent extract itself was colourless and no components which would explain the red appearance of the sediment sample could be identified by GC-MS. In order to rule out the possibility of the substance responsible for the colour

of the sample being physically or chemically bound to sediment matrix, for example via ester linkages between acid residues and free hydroxyl groups present on mineral surfaces, the sediment sample was re-extracted with methanolic sulfuric acid which can disrupt such associations and release the bound molecules as methyl esters (Huseby and Ocampo 1997). The acid extraction did not produce a coloured extract. Thus, on the basis of its inconspicuous extractable lipid profile it appears that the red material owes its colour to an inorganic mineral colourant rather than an organic chromophore.

4 Summary and conclusions

Analysis of the sediments from the tomb provided intriguing information relating to the burial practice and ritual of the Monte Claro culture burial at Gannì. Furthermore, the impact of body decay on the matrix adjacent to the human remains was evident through alteration of the sediments.

4.1 Pedogenesis associated with the human remains

Consistent with the tentative on-site archaeological interpretation, the lithified debris lying on the bone surface is attributed to material that had fallen from the vault of the chamber rather than being brought from elsewhere and lain on the skeleton for ritual or other purposes. Pedogenesis was pronounced only in the material that directly interacted with the organic matter from the body, both in the debris covering the remains and within the upper *c.* 10 mm of the resting plane under the skeletal remains. The similar organic carbon contents and compositions of these samples and the marl indicates that the organic components of the body tissues have degraded to below detectable limits within the burial chamber where the remains were exposed to the air. Thus, despite the complete degradation of the organic remains the pedogenic alteration of the sediment adjacent to the remains provides evidence of *in situ* decomposition of the body.

4.2 Calcium carbonate depletion from body decomposition

Pedofeature T, in the thigh and pelvic regions and in Context 32 containing the red concentrates, is a depletion pedofeature characterized by a significant loss of $CaCO_3$, small decrease in Mg and consequent relative increase in Fe levels compared with the surrounding grey matrix. Although sporadic patches of carbonate depletion occur in most samples, depletion features were considerably more abundant beneath the thigh and pelvic regions reaching ≥ 50% area within the uppermost 10 mm of the resting platform. The decalcification is attributed to localised acidification resulting from the generation of organic acids during body decomposition (Dent et al. 2004). Subject to the sediment matrix containing carbonates, such evidence could be of value in recognising primary burials in cases where skeletal articulation can not be established.

4.3 Ochre coloured context (Context 32)

The red haematite concentrates in Context 32, representing *c.* 10% by area of the disturbed/debris layer at the surface of the resting platform, were mixed with deposits that otherwise have very similar chemical compositions (with the exception of P and S) to the marl of the vault. The low organic matter content confirms the inorganic nature of Context 32. The extreme Fe concentrations in some regions, and high variability, reflect the heterogeneity observed by micromorphology. The Fe concentrations are well within the range recorded elsewhere for ochre type deposits (Attard Montalto et al. 2012; Gialanella et al. 2011; Iriarte et al. 2009; Popelka-Filcoff et al. 2008; Ramos et al. 2008). The heterogeneous mixture of haematite, silicates, clays and carbonates is also consistent with the previous analyses of archaeological ochre pigments (Darchuk et al. 2010; Gialanella et al. 2011). At other sites in Sardinia (Monte Claro culture: Sibiola, Su Fraigu (S. Sperate) and Sa Costa) and a Neolithic site at Ozieri (Manunza 2010a, 2010b) ochre was used for grave paintings and to adorn the dead. At Sibiola (16 km N of Gannì), ochre was used for single inhumations of elderly women, in tombs of identical architecture to those at Gannì. Thus, the identification of ochre deposits at Gannì, applied to a specific area of the grave as part of the burial ritual, complements and extends previous interpretations.

4.4 Grey fibrous material: torches from sedge

The grey fibrous material of the thin sub-circular lens of Tomb II and the clump to the side of the skeleton in Tomb I contained plant remains from the leaf and flower parts of non-cultivated herbaceous materials of the order Poales. Though almost entirely silicified, the material showed poorly ordered crystal form. The grey material from Tomb II (Context 28) contained plant-derived lipid components including a series of 5-*n*-alkylresorcinols. This supports the evidence from archaeobotanical analysis that the deposit relates to degraded plant material and suggests that it was deliberately placed in the tomb, probably as part of the burial ritual. In combination with the archaeobotanical evidence, the 5-*n*-alkylresorcinols provide compelling evidence for the material being from sedge. Analogous to elsewhere, it is suggested that silicification was induced during combustion. The rapid accumulation of the material *in situ* strongly suggests it was burnt in the burial chamber, though combustion was incomplete enabling some organic signatures to preserve. Given that the only access to the tombs at the time of burial was through a *c.* 3 m long vertical tunnel, it is likely that the grey fibrous materials derive from remains of torches fabricated from sedge, incomplete combustion possibly being associated with a tightly bound area. No other comparable contexts or other evidence for the use of torches exist in burials of the Monte Claro culture, nor is it known how these people illuminated their dwellings and caves.

The use of torches within the tombs could have been either for practical purposes or as part of a burial ritual. There is scant evidence of votive or ritual burning at other sites of the Monte Claro culture. Hypotheses of ritual burning for the dead were proposed on the basis of the presence of pieces of burnt wood found among grave goods adjacent to the dead in a cist (Gemiliano site) and the presence of some 5-8 cm vessels, considered to be either ointment holders or lamps, found near cremated or semi-combusted human bones in a disturbed cave (Tanì site). No information or further evidence to support the hypotheses is available (Lilliu 1998). In both cases, it is likely that those who sculpted the vaults and buried the dead needed light to illuminate the tombs during their passage, to carry the dead into the deep (3 m) and dark underground chambers and to prepare the burials with ochre and grave offerings for the dead. It is reasonable to assume that as the living withdrew from the tombs they left the torches in place, most likely as a votive offering to provide light for the dead.

Acknowledgements

This article is dedicated in memory of Maria-Raimonda Usai. The research forms part of the *InterArChive* project and has received funding from the European Research Council under the European Community's Seventh Framework Programme (FP7/2007-2013) / ERC grant agreement n° 230193. Allan Hall is thanked for archaeobotanical analysis, David Broughton for assistance with plant photomicrography and Karl Heaton for acquiring the GC-MS data.

References

Attard Montalto, N., Shortland, A., & Rogers, K. (2012). The provenancing of ochres from the Neolithic Temple Period in Malta. *Journal of Archaeological Science*, *39*(4), 1094–1102. doi:10.1016/j.jas.2011.12.010

Avsejs, L. A., Nott, C. J., Xie, S., Maddy, D., Chambers, F. M., & Evershed, R. P. (2002). 5-*n*-Alkylresorcinols as biomarkers of sedges in an ombrotrophic peat section. *Organic Geochemistry*, *33*(7), 861–867. doi:10.1016/S0146-6380(02)00046-3

Burns, A., Pickering, M. D., Green, K. A., Pinder, A. P., Gestsdóttir, H., Usai, M.-R., et al. (2017). Micromorphological and chemical investigation of late-Viking age grave fills at Hofstaðir, Iceland. *Geoderma*, *306*, 183–194. doi:10.1016/j.geoderma.2017.06.021

Carmignani, L., Oggiano, G., Funedda, A., Conti, P., Pasci, S., & Barca, S. (2012). *Carta Geologica della Sardegna. Scala 1:250.000*. (S. G. Italiano, Ed.). Firenze: Litografia Artistica Cartografica.

Chen, Y., Ross, A. B., Åman, P., & Kamal-Eldin, A. (2004). Alkylresorcinols as markers of whole grain wheat and rye in cereal products. *Journal of Agricultural and Food Chemistry*, *52*(26), 8242–8246. doi:10.1021/jf049726v

Darchuk, L., Tsybrii, Z., Worobiec, A., Vázquez, C., Palacios, O. M., Stefaniak, E. A., et al. (2010). Argentinean prehistoric pigments' study by combined SEM/EDX and molecular spectroscopy. *Spectrochimica Acta - Part A: Molecular and Biomolecular Spectroscopy*, *75*(5), 1398–1402. doi:10.1016/j.saa.2010.01.006

446 Dent, B. B., Forbes, S. L., & Stuart, B. H. (2004). Review of human decomposition processes in soil.
447 *Environmental Geology*, *45*(4), 576–585. doi:10.1007/s00254-003-0913-z

448 Drees, L. R., Wilding, L., Smeck, N. E., & Senkayi, A. L. (1992). Silica in soil: quartz and disordered silica
449 polymorphs. In J. N. Dixon & S. B. Weed (Eds.), *Minerals in Soil Environments*. Madison: Soil
450 Science Society of America.

451 Eglinton, G., & Hamilton, R. J. (1967). Leaf epicuticular waxes. *Science*, *156*(3780), 1322–1335.
452 doi:10.1126/science.156.3780.1322

453 Gialanella, S., Belli, R., Dalmeri, G., Lonardelli, I., Mattarelli, M., Montagna, M., & Toniutti, L. (2011).
454 Artificial or natural origin of hematite-based red pigments in archaeological contexts: The case
455 of Riparo Dalmeri (Trento, Italy). *Archaeometry*, *53*(5), 950–962. doi:10.1111/j.1475-
456 4754.2011.00594.x

457 Hall, A. R., & Huntley, J. P. (2007). *A review of the evidence for macrofossil plant remains from*
458 *archaeological deposits in Northern England* (Report Ser.). English Heritage Research
459 Department.

460 Huseby, B., & Ocampo, R. (1997). Evidence for porphyrins bound, via ester bonds, to the Messel oil
461 shale kerogen by selective chemical degradation experiments. *Geochimica et Cosmochimica*
462 *Acta*, *61*(18), 3951–3955. doi:10.1016/S0016-7037(97)00194-4

463 Iriarte, E., Foyo, A., Sánchez, M. A., Tomillo, C., & Setién, J. (2009). The origin and geochemical
464 characterization of red ochres from the Tito Bustillo and Monte Castillo Caves (Northern Spain).
465 *Archaeometry*, *51*(2), 231–251. doi:10.1111/j.1475-4754.2008.00397.x

466 Jambu, P., Amblès, A., Jacquesy, J.-C., Secouet, B., & Parlanti, E. (1993). Incorporation of natural
467 alcohols from plant residues into hydromorphic forest-podzol. *Journal of Soil Science*, *44*(1), 135–
468 146. doi:10.1111/j.1365-2389.1993.tb00440.x

469 Kozubek, A., & Tyman, J. H. P. (1999). Resorcinolic lipids, the natural non-isoprenoid phenolic
470 amphiphiles and their biological activity. *Chem. Rev.*, *99*(1), 2–25. doi:10.1021/cr970464o

471 Lagerås, P. (2000). Burial rituals inferred from palynological evidence: results from a late Neolithic
472 stone cist in southern Sweden. *Vegetation History and Archaeobotany*, *9*, 169–173.
473 doi:10.1007/BF01299801

474 Lilliu, G. (1998). *La Civilta dei Sardi - dal Paleolitico all'eta dei nuraghi* (3rd ed.). Torino: Nuova ERI.

475 Manunza, M. R. (2010a). Serdiana, Sibiola tomba II. In M. R. Manunza (Ed.), *Bau su Matutzu Serdiana:*
476 *segni del potere in una sepoltura del III millennio a.C., Cagliari*. Cagliari: Scuola Sarda Editrice.

477 Manunza, M. R. (2010b). Settimo S. Pietro, Sa Costa is Crus tomba 40. In M. R. Manunza (Ed.), *Bau su*
478 *Matutzu Serdiana: segni del potere in una sepoltura del III millennio a.C., Cagliari*. Cagliari: Scuola
479 Sarda Editrice.

480 Manunza, M. R. (2013). Corredi funerari di cultura Monte Carlo a Gannì (Quartucciu - CA). *Notizia*
481 *preliminare, Quaderni Soperintendenza per i Beni Archaeologici delle province di Cagliari e*
482 *Oristano*, *24*, 39–76.

483 Mattila, P., Pihlava, J. M., & Hellström, J. (2005). Contents of phenolic acids, alkyl- and
484 alkenylresorcinols, and avenanthramides in commercial grain products. *Journal of Agricultural*
485 *and Food Chemistry*, *53*(21), 8290–8295. doi:10.1021/jf051437z

Munsell. (2009). *Munsell Soil Colour Charts*. New Windsor, NY, USA: Macbeth, Division of Kollmorgen Instruments Corporation.

Pickering, M. D., Ghislandi, S., Usai, M.-R., Wilson, C., Connelly, P., Brothwell, D. R., & Keely, B. J. (2018). Signatures of degraded body tissues and environmental conditions in grave soils from a Roman and an Anglo-Scandinavian age burial from Hungate, York. *Journal of Archaeological Science*, *99*, 87–98. doi:10.1016/j.jas.2018.08.007

Pickering, M. D., Lang, C., Usai, M.-R., Keely, B. J., & Brothwell, D. R. (2014). Organic residue analysis of soils. In L. Loe, A. Boyle, H. Webb, & D. Score (Eds.), *"Given to the ground": a Viking age mass grave on Ridgeway Hill, Weymouth* (pp. 237–245). Dorset Natural History and Archaeological Society Monograph Series Vol 23, Oxbow Books Oxford.

Popelka-Filcoff, R. S., Miksa, E. J., Robertson, J. D., Glascock, M. D., & Wallace, H. (2008). Elemental analysis and characterization of ochre sources from Southern Arizona. *Journal of Archaeological Science*, *35*(3), 752–762. doi:10.1016/j.jas.2007.05.018

Ramos, P. M., Ruisánchez, I., & Andrikopoulos, K. S. (2008). Micro-Raman and X-ray fluorescence spectroscopy data fusion for the classification of ochre pigments. *Talanta*, *75*(4), 926–936. doi:10.1016/j.talanta.2007.12.030

Robinson, M. A., & Straker, V. (1991). Silica skeletons of macroscopic plant remains from ash. In J. M. Renfrew (Ed.), *New Light on Early Farming. Recent Developments in Palaeoethnobotany*. Edinburgh: University Press.

Roebroeks, W., Sier, M. J., Nielsen, T. K., De Loecker, D., Pares, J. M., Arps, C. E. S., & Mucher, H. J. (2012). Use of red ochre by early Neandertals. *Proceedings of the National Academy of Sciences*, *109*(6), 1889–1894. doi:10.1073/pnas.1112261109

Ross, A. B., Shepherd, M. J., Schüpphaus, M., Sinclair, V., Alfaro, B., Kamal-Eldin, A., et al. (2003). Alkylresorcinols in cereals and cereal products. *Journal of Agricultural and Food Chemistry*, *51*(14), 4111–4118. doi:10.1021/jf0340456

Ugas, G. (1993). S. Sperate - Su Fraigu tomba 13, Cagliari, tav. LIV. In G. Ugas (Ed.), *San Sperate dalle origini ai baroni*. Cagliari: Della Torre Cagliari.

Usai, M.-R., Pickering, M. D., Wilson, C. A., Keely, B. J., & Brothwell, D. R. (2014). 'Interred with their bones': soil micromorphology and chemistry in the study of human remains. *Antiquity. Project Gallery*, *88*, 339.

Zarnowski, R., & Kozubek, A. (1999). Alkylresorcinol homologs in Pisum sativum L. varieties. *Zeitschrift fur Naturforschung*, *54c*(1–2), 44–48.